# Insights Into Heat Response Mechanisms in Clematis Species: Physiological Analysis, Expression Profiles and Function Verification

**Hao Zhang**
Shanghai Normal University - Xuhui Campus: Shanghai Normal University
**Changhua Jiang**
Shanghai Botanical Garden
**Rui Wang**
Shanghai Normal University - Xuhui Campus: Shanghai Normal University
**Long Zhang**
Shanghai Normal University - Xuhui Campus: Shanghai Normal University
**Ruonan Gai**
Shanghai Normal University - Xuhui Campus: Shanghai Normal University
**Siyuan Peng**
Shanghai Normal University - Xuhui Campus: Shanghai Normal University
**Yi Zhang**
Shanghai Normal University - Xuhui Campus: Shanghai Normal University
**Chanjuan Mao**
Shanghai Normal University - Xuhui Campus: Shanghai Normal University
**Yuxia Lou**
Shanghai Normal University - Xuhui Campus: Shanghai Normal University
**Jianbin Mo**
Shanghai Botanical Garden
**Shucheng Feng**
Shanghai Botanical Garden
**Feng Ming** ( ZH20190303@163.com )
Shanghai Normal University https://orcid.org/0000-0003-1788-6218

**Research Article**

**Keywords:** Clematis, Heat stress, Transcriptome, HSFs, HSPs, VIGS

**Posted Date:** March 26th, 2021

**DOI:** https://doi.org/10.21203/rs.3.rs-338667/v1



**Version of Record:** A version of this preprint was published at Plant Molecular Biology on July 14th, 2021. See the published version at https://doi.org/10.1007/s11103-021-01174-4.

# Abstract

*Clematis* species are commonly grown in western and Japanese gardens. Heat stress can inhibit many physiological processes mediating plant growth and development. The mechanism regulating responses to heat has been well characterized in *Arabidopsis thaliana* and some crops, but not in horticultural plants, including *Clematis* species. In this study, we found that *Clematis alpina* 'Stolwijk Gold' was heat-sensitive whereas *Clematis vitalba* and *Clematis viticella* 'Polish Spirit' were heat-tolerant based on the physiological analyses in heat stress. Transcriptomic profiling identified a set of heat tolerance-related genes (HTGs). Consistent with the observed phenotype in heat stress, 41.43% of the differentially expressed HTGs between heat treatment and control were down-regulated in heat-sensitive cultivar Stolwijk Gold, but only 9.80% and 20.79% of the differentially expressed HTGs in heat resistant *C. vitalba* and Polish Spirit, respectively. Co-expression network, protein–protein interaction network and phylogenetic analysis revealed that the genes encoding heat shock transcription factors (HSFs) and heat shock proteins (HSPs) played an essential role in *Clematis* resistance to heat stress. Ultimately, we proposed that two clades of HSFs may have diverse functions in regulating heat resistance from *C. vitalba* and *CvHSFA2-2* could endow different host with high temperature resistance. This study provides first insights into the diversity of the heat response mechanisms among *Clematis* species.


# Introduction

*Clematis* is a genus that includes approximately 300 species belonging to the buttercup family (Ranunculaceae). *Clematis* species play an important role in western and Japanese gardens, and are commonly grown in botanical gardens, parks, and family gardens. However, the growth of some *Clematis* varieties is restricted because of their sensitivity to heat and increasing global warming. To date, most researches related to *Clematis* species have been focused on taxonomy and ecology (Wanasinghe et al. 2014; Picciau et al. 2017; Paynter et al. 2006; Redmond and Stout 2018).

Environmental changes have a broad arrange of influences on plant growth and development. For example, high temperatures lead to various changes of plant morphology including elongation of the hypocotyl and petiole, early flowering, and reduced stomata number (Li et al. 2018a). How plant cells perceive the thermal signal remains unclear (Zhang et al. 2019), although previous research has identified thermosensors such as H2A.Z-containing nucleosomes and phytochromes (Legris et al. 2016). Nevertheless, some key factors involved in heat-shock signal transduction were identified (Ding et al. 2020), for example, a heat activated calcium channel AtCNGC8 is involved in heat shock responses (Gao et al. 2012), molecular and genetic evidence support that AtCaM3 also plays a crucial part in heat-shock signal transduction in Arabidopsis (Liu et al. 2008; Zhang et al. 2009).

Heat stress can adversely affect plant protein structure, conformation, and activity, resulting in denatured and aggregated proteins as well as plant cell death due to biochemical damages and cytotoxicity (Li et al. 2018a; Zhang et al. 2019). Heat shock proteins (HSPs) are molecular chaperones that can stabilize and degrade unfolded proteins (Hendrick and Hartl 1993). Heat stress significantly increases the production of HSP90, which directly interacts with TRANSPORT INHIBITOR RESPONSE 1 (TIR1) to prevent protein degradation and regulate auxin-mediated plant growth (Wang et al. 2016). Heat shock transcription factors (HSFs) are conserved and have central roles in transcriptional regulation of plant thermotolerance. The *A. thaliana* genome encodes 21 HSFs, which have been divided into three classes: HSFA, HSFB, and HSFC (Scharf et al. 2018). It has been shown that decreased expression of these genes, such as *HSFA2*, *HSFA3* and *HSFB1* via T-DNA insertions or RNA interference significantly alters plant thermotolerance (Schramm et al. 2008; Ikeda et al. 2011; Liu et al. 2011; Liu and Charng 2013; Huang et al. 2016; Fang et al. 2015). In addition to HSFs, other transcription factors were also reported to be responsive to heat stress. For example, emerging evidence indicates that *DREB2A* also plays a critical role in heat stress tolerance (Liu et al. 1998), *OsSNAC3* expression is induced within a few hours of an exposure to heat and salt stresses, and the encoded protein regulates reactive oxygen species (ROS) homeostasis by directly activating many genes related to ROS clearance (Fang et al. 2015). Excess ROS which are produced under heat stress are also toxic to plants (Ding et al. 2020). A previous study revealed that OsANN1 is a calcium-binding membrane-bound protein that regulates $H_2O_2$ production by promoting the activities of superoxide dismutase and catalase, thereby making rice resistant to high temperatures (Qiao et al. 2015). In addition to its effects on transcription, protein homeostasis and ROS homeostasis, thermal stress also influences other nuclear regulatory processes, including

chromatin modification, remodeling, and RNA processing (Li et al. 2018b; Kumar et al. 2012; Kumar and Wigge 2010; Zhang et al. 2019). However, the mechanism underlying heat resistance of horticultural plant species has not been characterized yet.

In this study, by comparing the primary heat-related physiological indices before and after a high-temperature treatment, we identified a heat-sensitive *Clematis* variety (*Clematis alpina* 'Stolwijk Gold') and two heat-tolerant *Clematis* varieties (*Clematis vitalba* and *Clematis viticella* 'Polish Spirit'). We also analyzed the transcriptomes of these varieties under normal and heat stress conditions. GO enrichment analyses revealed that heat stress mainly influences components of biological membrane and two heat-tolerant *Clematis* varieties have obvious positive regulation to heat stress whereas the heat-sensitive *Clematis* variety does not. Moreover, we compared the varieties regarding their responses to heat to clarify the differences in their heat resistance. Furthermore, we identified two HSF classes with potential different functions related to heat resistance and verified that *CvHSFA2-2* enhanced the viability of *E. coli*, yeast and tobacco to survive in thermal stress. The results of this study provide insights into the diversity of the heat response mechanisms among *Clematis* species and may be useful for breeding new heat-resistant ornamental *Clematis* varieties.

## Materials And Methods

# Plant material growth conditions and high temperature treatment conditions

Triennial potted plants (40 cm high) of three *Clematis* varieties (*Clematis vitalba*, Polish Spirit and Stolwijk Gold) were used in this study. Their seeds were derived from France Botanical Garden (France Jardin Botanique, 44094 Nantes cedex 1, 47°22'N, 1°55'W), which were sown into autoclaved nutrient soil and grown for 3 years in 12-inch pots in greenhouse (25/20°C day/night, 70% relative humidity, 14-h/10-h light/dark cycles) of Shanghai Botanical Garden (Shanghai, China, 31°09'N, 121°26'E). Experimental treatments and sample collection were conducted in July 5th, 2019 in Shanghai Botanical Garden. For each variety, eighteen plants randomly selected from one hundred potted plants with great and similar growth condition grown in the greenhouse were used and treated at 38℃ (treatment) and 22 ℃ (control) for 3 hours, respectively (nine plants at every temperature). Each temperature treatment was performed and repeated in three growth chambers (38℃, 70% relative humidity or 22℃, 70% relative humidity). The leaves of treated potted plants were used subsequent physiological indexes analysis and RNA sequencing. The high temperature treatment of transgenic tobacco was consistent with the above methods.

# Measurement of physiological indexes before and after high temperature treatment

For measurement of relative conductivity (RC), Leaves (0.2 g) were collected, rinsed three times using distilled water, and then placed into a 50 ml tubes with 30 ml distilled water. Initial conductivity (Ci) was measured using a conductivity meter (DDS-11A, Shanghai, China) after shaking for 24 h. The samples were then autoclaved for 30 min. The maximum conductivity (Cmax) was quantified when the tubes were cooled to room temperature. The RC was calculated as (Ci/Cmax) × 100%. For relative water content (RWC) quantification, approximately 0.2 g fresh leaves were collected at each variety and immediately weighed as the fresh weight (FW). Leaf samples were then placed in an oven at 80°C for 72 h prior to being weighted for dry weight (DW). The RWC was subsequently calculated using the following equation: RWC (%) = [(FW– DW) / FW] × 100% (Flexas et al. 2006). The activity of SOD was quantified using an enzyme-linked immunosorbent assay (ELISA) kit (MSKBIO, China) following the manufacturer's instructions. The MDA contents were measured with the thiobarbituric acid (TBA) chromatometry method (Bao et al. 2019). Leaf samples (0.5 g) were ground into a homogenate with 5 ml 10% trichloroacetic acid (TCA) solution. After centrifugation at 4000 rpm for 10 min, 2 ml of the supernatant was transferred to tubes and mixed with 2 ml 0.6% TBA solution. The mixture was immersed in boiling water for 15 min and then quickly cooled to room temperature. The absorbance at 450, 532 and 600 nm was then measured using Nanodrop2000. The content of soluble protein was determined by the Coomassie brilliant blue method (Bao et al. 2020). 0.1 g of leaves were ground into a homogenate with deionized water (5 ml), which was subsequently centrifuged for 10 min at 3000 rpm. One millilitre of the supernatant was transferred to a test tube and diluted 5 times with deionized water (4 ml). One millilitre of the diluted solution was mixed with 5 ml of Coomassie brilliant blue G-250 (Shanghai Huishi Biochemical Reagent Co., Ltd). The absorbance was measured at 595 nm after 2 min with Nanodrop2000,

and the protein content was determined via a standard curve. Three biological replicates were performed for measurement of every physiological index.

# Nitro blue tetrazole (NBT) and Diaminobenzidine (DAB) staining

Leaves of three Clematis varieties and tobacco with normal and high temperature treatment were soaked in DAB staining solution at 25°C for 24 hours or NBT staining solution at 25°C for 12 h both in the dark according to previously reported method (Cen et al. 2018), and then soaked in 95% ethanol to remove chlorophyll and took the photo.

# RNA isolation and sequencing

Eighteen samples (Cv_NT_leaf1, Cv_NT_leaf2, Cv_NT_leaf3, Cv_HT_leaf1, Cv_HT_leaf2, Cv_HT_leaf3, PS_NT_leaf1, PS_NT_leaf2, PS_NT_leaf3, PS_HT_leaf1, PS_HT_leaf2, PS_HT_leaf3, SG_NT_leaf1, SG_NT_leaf2, SG_NT_leaf3, SG_HT_leaf1, SG_HT_leaf2 and SG_HT_leaf3) from three Clematis varieties were used for RNA sequencing. For each variety, every sample was collected quickly stored at − 80°C after frozen in liquid nitrogen from leaves of three plants treated in different growth chambers after 38℃ or 22℃ treatment. RNA was isolated using TRIzol reagent, respectively. The extracted RNA was quantified using Nanodrop2000, and the RNA was electrophoresed on an agarose gel to check its integrity. Around 0.4 μg of total RNA was used for library construction and sequencing on an Illumina Novaseq 6000 (Illumina, San Diego, CA, USA) at Shanghai Majorbio Bio-pharm Technology Co.,Ltd (Shanghai, China). Prior to library construction, an Agilent 2100 Bioanalyzer (Agilent, CA, USA) was used to confirm the quality and quantity of RNA such that the rRNA ratio (28 s/18 s) was > 1.5 and the RNA integrity number > 7. In brief, 0.1 ~ 0.4 μg total mRNA was purified and fragmented using PCR plates with a magnetic plate stand. Fragmented mRNA was reverse-transcribed to cDNA using random primers and Superscript II (Invitrogen, Carlsbad, CA). Blunt-ended cDNA was generated by end repair and then ligated to yield 30 adenine base overhangs. Oligonucleotide adapters with thymine overhangs were ligated to the cDNA and added to the adapter index for each library. The library fragments were enriched by PCR amplification and ~ 895 million raw pair-end reads were generated on an Illumina Novaseq 6000.

**Trimming**, de novo **assembly and mapping of reads**

Illumina sequence data were assessed using fastx_toolkit_0.0.14 (http://hannonlab.cshl.edu/fastx_toolkit/) and filtered using SeqPrep (https://github.com/jstjohn/SeqPrep) and Sickle (https://github.com/najoshi/sickle). All clean reads of each *Clematis* variety were used *de novo* assembly using Trinity (https://github.com/trinityrnaseq/trinityrnaseq). Assembly results were optimized using TransRate (http://hibberdlab.com/transrate/) and CD-HIT (http://weizhongli-lab.org/cd-hit/) and then assessed using BUSCO (Benchmarking Universal Single-Copy Orthologs, http://busco.ezlab.org). Clean reads of every samples were respectively mapped to *de novo* assemble sequence.

# Transcriptome annotation, identification and enrichment analysis of differential expressed genes (DEGs)

Transcriptome assembly sequences were annotated by NR (ftp://ftp.ncbi.nlm.nih.gov/blast/db/),Swiss-Prot (http://web.expasy.org/docs/swiss-prot_guideline.html), Pfam (http://pfam.xfam.org/), COG (Clusters of Orthologous Groups of proteins, http://www.ncbi.nlm.nih.gov/COG/), GO (Gene Ontology, http://www.geneontology.org) and KEGG (Kyoto Encyclopedia of Genes and Genomes, http://www.genome.jp/kegg/) six databases, respectively. Gene expression levels were calculated as transcripts per million reads (TPM) using RSEM (http://deweylab.github.io/RSEM/). Differential expressed genes (DEGs) in three Clematis varieties were identified using DEseq2 (|log2 FC(HT_leaf/NT_leaf)|>2, p-value < 0.05). The software Goatools was used for GO enrichment analysis (FDR < 0.05) of DGEs with Fisher's exact test. All of the DEGs were also subjected to KOBAS 2.0 analysis (http://kobas.cbi.pku.edu.cn/home.do) and significant pathways were selected at a corrected p value < 0.05.

# Hierarchical cluster analysis

The hierarchical clustering and other statistical analyses were carried out using R software (http://www.r-project.org). Pearson correlation was used to calculate distance of different samples.

# Identification of heat tolerance-related genes

On the one hand, we obtained protein sequences based on transcriptome assembly sequence using Transdecoder (https://github.com/TransDecoder) and construct local protein databases of three *Clematis* varieties. Then proteins homologous with previously reported heat tolerance-related genes (HTGs) (Supplementary Table 6) were identified using the local blastp program of BLAST + 2.9.0 (ftp://ftp.ncbi.nlm.nih.gov/blast/executables/blast+/LATEST/) (E-value < 1e-5, identity > 60%) in three *Clematis* varieties. On the other hand, genes of GO term related to heat-resistance in GO enrichment analysis were also regarded as heat-tolerant genes (HTGs). We combined both data to define heat tolerance-related genes (HTGs) (Supplementary Table 7) in three *Clematis* varieties, respectively.

# Differentially expressed analysis of heat tolerance-related genes

TPM data of the overlap between DGEs and HTGs, that is, expression profiles of differentially expressed HTGs were visualized in R software (https://www.r-project.org/). Blue and red represented “down regulated” and “up regulated”, respectively.

# Construction of co-expression network and protein-protein interaction network

We used differentially expressed HTGs for further network construction. Co-expression correlation coefficients of differentially expressed HTGs were obtained through Spearman algorithm (corrected p value < 0.05) based on gene expression data using R software (http://www.r-project.org) and visualized in Cytoscape v3.5.1 (Shannon et al. 2003). PPI networks of differentially expressed HTGs were constructed based on PPIs of *Aquilegia coerulea* in STRING database (https://string-db.org) for three *Clematis* varieties. Networks were also visualized using Cytoscape v3.5.1. Number of edges directly connected with nodes were computed using Network Analyzer in Cytoscape v3.5.1 (Assenov et al. 2008).

# Phylogeny and expression analysis of HSFs and HSPs

Phylogenetic trees of HSFs and HSPs from three *Clematis* species were constructed in IQ-TREE v2.0.6 (Minh et al. 2020) with JTT + I + G4 and VT + R3 model respectively. Support for each node was assessed by performing a bootstrap analysis with 1000 replicates. The phylogenetic analysis of HSFs from *Clematis vitalba* and *Arabidopsis thaliana* was inferred by using the Maximum Likelihood method based on the JTT matrix-based model in MEGA-X (Kumar et al. 2018; Jones et al. 1992). The bootstrap consensus tree inferred from 1000 replicates is taken to represent the evolutionary history of the taxa analyzed (Felsenstein 1985). Fewer than 5% alignment gaps, missing data, and ambiguous bases were allowed at any position (partial deletion option). Expression profiles (TPM data) of differential expressed HSFs and HSPs were visualized in iTOL (https://itol.embl.de/). Green and red represented “down regulated” and “up regulated” respectively.

# Motif prediction and visualization of HSFs

Motif prediction and visualization of CvHSFA2-1, CvHSFA2-2 and CvHSFB2b were performed in HEATSTER (https://applbio.biologie.uni-frankfurt.de/hsf/heatster/home.php).

# RNA extraction and quantitative real-time PCR assay

Total RNA was extracted with TRIzol Reagent from leaves of *Clematis vitalba* grown under the normal condition and high temperature treatments with 0.5h, 1h, 1.5h and 2h. The cDNA was synthesized using the PrimeScript RT Reagent Kit with gDNA Eraser (Takara, Kyoto, Japan). PCR amplifications were performed using the TransStart Tip Green qPCR SuperMix (TransGen Biotech, Beijing, China) on the CFX96™ Real-Time PCR Detection System (Bio-Rad, Hercules, CA, USA). Gene-specific primers used in the experiments are listed in Supplementary Table 8. Real-time PCRs were done on a Chromo 4™ continuous fluorescence detector with the SYBR RT-PCR Kit (Takara), in a 20μl reaction volume, which contained 10 μl of SYBR Green I PCR mix, 0.5μM of each forward and reverse primer, 1μl of cDNA template, and appropriate amounts of sterile dd$H_2O$. Amplification conditions were: 2 min at 95℃; 40 cycles of 15 s at 95℃, 30 s at 58℃, and 30 s at 72℃. Fold changes of RNA transcripts were calculated by the $2^{-\Delta\Delta Ct}$ method (Livak and Schmittgen 2001) with *CvUBC2D* as an internal control. The entire experiments were repeated three times.

# Functional verification of prokaryotic host

The open reading frame (ORF) of *CvHSFA2-2* was amplified by the primers in Table S8, and the fragment was cloned into the corresponding restriction sites of pET28a and confirmed by DNA sequencing. The plasmid was then transformed into *E. coli* BL21 (DE3) strain by heat shock method. A strain only transformed with plasmid PET-28a was used as a negative control. For thermotolerance assays, *E. coli* cell cultures were grown at 37°C to optical density at 600 nm (OD600) of 1.0 and then diluted once with fresh Luria-Bertani (LB) medium supplemented with ampicillin (100 mg mL-1) and isopropyl-beta-D-thiogalactopyranoside (IPTG; 0.5 mM). Cultures were shifted to 42℃ and 50°C after 2 h of IPTG induction. Serial dilutions were plated in triplicate and cell viability was measured by counting colony-forming units in triplicate plates.

# Functional verification of eukaryotic host

The recombinant composed of the *CvHSFA2-2* gene fragments and the pGADT7 vector was amplified using the primers in Table S8 and transferred into the eukaryotic yeast AH109 by PEG/LiCl method. The strain only transformed with plasmid pGADT7 was used as a negative control. AH109 recombinant cells were pre-cultivated aerobically for 12–14 h in SD/-Leu medium (28°C, 250 rpm) to OD600 of 1.0-1.8. The cultures were centrifuged and washed once with 1X phosphate-buffered solution (PBS) and then inoculated in SD/-Leu medium of which the initial OD600 was adjusted to 0.05 and cultivated with a speed of 250 rpm at 28°C, 37°C or 42°C for 12h. In addition, 5 µL AH109 liquid from each treatment were drop on triplicate SD/-Leu medium and incubated at 28°C for 2–3 d. Cell concentrations were calculated by optical density (OD600) spectrophotometric measurements.

# Functional verification of VIGS with tobacco as host

For tobacco VIGS assay(Zhang et al. 2017), part of the homologous nucleotide sequence of *CvHSFA2-2* was separately linked to pTRV2 virus vector. The constructed pTRV2 vectors mentioned above were introduced into *A. tumefaciens* strain GV3101. Agrobacterium harboring TRV1 or TRV2 derivative vectors were mixed at 1:1 ratio and infiltrated into the leaves of 2-week-old *N. benthamiana* plants. The newly growing leaves were used for heat tolerance access and silence effect identification two weeks after injection.

## Results

### Heat shock phenotype of different Clematis varieties

*Clematis vitalba* (Cv) is an original *Clematis* specie that produces branched and grooved stems as well as deciduous leaves and green-white flowers with fluffy underlying sepals. Because of its disseminatory reproductive system, vitality, and climbing behavior, *C. vitalba* is an invasive plant species in several regions, including New Zealand (http://www.iucngisd.org/gisd/species.php?sc=157). ‘Polish Spirit’ (PS) and ‘Stolwijk Gold’ (SG) are ornamental *Clematis* cultivars recognized by the Royal Horticultural Society of England (http://apps.rhs.org.uk/advicesearch/profile.aspx?pid=97).

To compare the heat resistance of three *Clematis* varieties, we observed heat shock phenotype of three Clematis varieties and analyzed several physiological parameters of the leaves from the plants treated with or without high-temperature (HT) treatment (Fig. 1, Supplementary Table 1). After heat treatment (38℃ for 3h), Stolwijk Gold appeared obvious leaf wilting whereas *Clematis vatalba* and Polish spirit not (Fig. 1a). Our data showed that the relative conductivity (RC) and malondialdehyde content were significantly higher in Stolwijk Gold than in *C. vitalba* and Polish Spirit, whereas the relative water content (RWC), soluble protein content, and superoxide dismutase activity (SOD) were lower in Stolwijk Gold than in *C. vitalba* and Polish Spirit (Fig. 1b). These results indicate that the heat-induced membrane damage and peroxidation were greater in Stolwijk Gold than in *C. vitalba* and Polish Spirit. Moreover, nitroblue tetrazolium and diaminobenzidine staining revealed that heat treatment led to the substantial accumulation of ROS in Stolwijk Gold leaves (Fig. 1c) but unchanged ROS content in *C. vitalba* and Polish Spirit, indicating that the antioxidant systems of Polish Spirit and *C. vitalba* remained active under heat stress conditions (Fig. 1d). These results reflected the heat resistance of *C. vitalba* and Polish Spirit as well as the sensitivity of Stolwijk Gold to heat stress.

### Effect of heat stress on transcriptomic profiles of Clematis species

To reveal the molecular basis of the differences in the heat resistance of the three *Clematis* varieties, the leaf transcriptomes under normal (control) and heat stress conditions were analyzed by RNA-sEq. Eighteen libraries corresponding to three

biological replicates for the control and heat treatments of each variety were constructed and sequenced. A total of approximately 895 million paired-end reads (raw reads) were generated, filtered, and trimmed, with 40–60 million reads per library (Supplementary Table 2). The raw data have been deposited in the NCBI Sequence Read Archive (PRJNA664279). For each *Clematis* variety, all clean reads were used for a *de novo* sequence assembly using Trinity (https://github.com/trinityrnaseq/trinityrnaseq) (Supplementary Table 3). The obtained unigenes for the three *Clematis* varieties were annotated based on the following six databases: NR (ftp://ftp.ncbi.nlm.nih.gov/blast/db/), Swiss-Prot (http://web.expasy.org/docs/swiss-prot_guideline.html), Pfam (http://pfam.xfam.org/), COG (Clusters of Orthologous Groups of proteins, http://www.ncbi.nlm.nih.gov/COG/), GO (Gene Ontology, http://www.geneontology.org), and KEGG (Kyoto Encyclopedia of Genes and Genomes, http://www.genome.jp/kegg/) (Supplementary Table 4). For each variety, approximately half of the unigenes matched *Aquilegia coerulea* sequences (Supplementary Fig. 1), reflecting the close genetic relationship between *Clematis* species and *A. coerulea*. The clean reads were then mapped to the assembled sequence (Supplementary Table 5). The gene expression levels (i.e., transcripts per million reads) were analyzed using RSEM (http://deweylab.github.io/RSEM/). The hierarchical cluster analysis of gene expression among the different samples for each variety indicated the data for the biological replicates were reliable and the error was within the allowable range (Fig. 2a). The expression profiles of differentially expressed genes (DEGs) among the three *Clematis* varieties were visualized (Fig. 2b, Supplementary Fig. 2). There were 5344, 5749 and 6506 DEGs in *C. vitalba*, Polish spirit and Stolwijk Gold under normal and high temperature, respectively, which accounted for 6.4%, 9.0% and 10.6% of the respective total unigenes of three varieties (Fig. 2c). The number of DEGs and the ratio of the number of DEGs to the total number of genes were highest for Stolwijk Gold, and lowest for *C. vitalba* (Fig. 2c), implying that more biological processes were affected by heat stress in Stolwijk Gold than in *C. vitalba* and Polish Spirit. The GO enrichment analyses of the DEGs revealed that the heat treatment mainly altered membrane components, with some DEGs in *C. vitalba* and Polish Spirit related to heat responses (Fig. 3), indicating that the two heat-tolerant Clematis varieties conducted positive and effective regulation resistant to heat stress. The KEGG pathway enrichment analysis indicated that the pathways affected by heat were mainly associated with secondary metabolism, with fewer pathways affected in *C. vitalba* than in the other examined varieties (Supplementary Fig. 3). Additionally, some signaling pathways in Stolwijk Gold were modulated by heat stress, including plant hormone signal transduction and the MAPK signaling pathway (Supplementary Fig. 3). These results suggest that *C. vitalba* and Polish Spirit are more heat resistant than Stolwijk Gold.

# Identification of heat tolerance-related genes and their differential expression

On the basis of previous research (Zhang et al. 2019; Li et al. 2018a; Ding et al. 2020), we found that there were some reported important genes (defined as heat tolerance-related genes in here) which have been verified to improved plant thermotolerance, 53 currently reported heat tolerance-related genes (HTGs) were carefully chosen in here that were involved in five regulatory processes mediating plant responses to high stress: heat signal transduction, transcriptional regulation, protein homeostasis, ROS homeostasis and RNA homeostasis (Supplementary Table 6). To further explain the difference in heat resistance of three analyzed *Clematis* varieties and elucidate their molecular mechanism underlying the heat responses, we identified the heat tolerance-related genes (HTGs) associated with the above-mentioned five regulatory categories in three varieties (Supplementary Table 7). It's worth noting that the HTGs of three varieties were identified via a local blastp search using 53 previously reported HTGs in other species as queries (Supplementary Table 6) and GO term annotations. Additionally, their expression levels in the three examined *Clematis* varieties were compared (Table 1, Fig. 4, Supplementary Table 7). Expression levels of some differentially expressed HTGs in each species were down-regulated. More specifically, 41.43% of the differentially expressed HTGs in Stolwijk Gold were significantly down-regulated under heat stress, whereas only 9.80% and 20.79% of the differentially expressed HTGs were down-regulated in *C. vitalba* and Polish Spirit, respectively (Fig. 4a). Polish Spirit had the most up-regulated HTGs. *Clematis vitalba* had the fewest down-regulated HTGs (Fig. 4a). These results may help to explain the heat resistance of *C. vitalba* and Polish Spirit.

Table 1

**Heat tolerance-related genes among different cellular processes and their differential expression under heat stress in three** Clematis **varieties.** Identified: all identified HTGs, differ: differentially expressed HTGs, up: up-regulated HTGs, down: down-regulated HTGs.

| Species | Cv | | | | PS | | | | SG | | | |
|---|---|---|---|---|---|---|---|---|---|---|---|---|
| | identified | differ | up | down | identified | differ | up | down | identified | differ | up | down |
| Heat Signal Transduction | 21 | 0 | 0 | 0 | 18 | 2 | 0 | 2 | 21 | 5 | 0 | 5 |
| Transcriptional Regulation | 41 | 11 | 9 | 2 | 43 | 18 | 13 | 5 | 49 | 13 | 6 | 7 |
| Protein Homeostasis | 227 | 40 | 37 | 3 | 220 | 77 | 66 | 11 | 275 | 46 | 33 | 13 |
| ROS Homeostasis | 11 | 0 | 0 | 0 | 20 | 3 | 0 | 3 | 19 | 6 | 2 | 4 |
| RNA Homeostasis | 1 | 0 | 0 | 0 | 1 | 1 | 1 | 0 | 1 | 0 | 0 | 0 |
| Total | 301 | 51 | 46 | 5 | 302 | 101 | 80 | 21 | 365 | 70 | 41 | 29 |

There were considerable differences in the expression of HTGs in the above-mentioned regulatory categories among the three *Clematis* species. Transcriptional regulation is critical for plant responses to high temperatures. The HSF family members as well as the ERF/AP2 family transcription factor DREB2A and the NAC transcription factor NAC019 positively affect the heat-activated transcriptional regulatory network (Sato et al. 2014; Guan et al. 2014). Genes encoding these transcription factors were identified in the *Clematis* transcriptomes (Fig. 4). In response to heat stress, all *HSF* genes identified in *C. vitalba* were significantly up-regulated, whereas only half of the *HSF* genes identified in Stolwijk Gold had up-regulated expression levels (the rest had down-regulated expression levels). Moreover, many of the *DREB2A* and *NAC019* transcription factor genes were expressed at lower levels in Stolwijk Gold than in the other varieties. We speculated that the sensitivity of Stolwijk Gold to heat is primarily due to a weak heat-activated transcriptional regulatory network. Additionally, maintaining homeostasis, especially related to protein and ROS contents, is extremely important for stabilizing the biological activities of plants exposed to heat stress (Li et al. 2018b; Zhang et al. 2019). Heat shock proteins, which are molecular chaperones, are important for the stabilization, renaturation, and degradation of unfolded proteins. Following the heat treatment, an analysis of the differentially expressed *HSP* genes indicated that Polish Spirit had the most up-regulated *HSP* genes, whereas *C. vitalba* had the highest proportion of up-regulated *HSP* genes (Fig. 4b). These findings may be related to the differences in the heat resistance mechanisms of the evaluated *Clematis* varieties. In plants, ROS accumulation is a major cellular response to heat stress. However, high ROS contents lead to the oxidative damage of many cellular components (Vacca et al. 2006; Petrov et al. 2015). The HTGs related to ROS homeostasis were not differentially expressed in *C. vitalba*, but had down-regulated expression levels in Polish Spirit after the high-temperature treatment (Table 1, Fig. 4b), indicating that the heat resistant mechanism prevents the excessive accumulation of ROS in *C. vitalba* and Polish Spirit. Although expression of the two HTGs related to ROS homeostasis was up-regulated in Stolwijk Gold, four other HTGs related to ROS homeostasis were down-regulated, indicative of ROS accumulation (Fig. 1c and d, Table 1, Fig. 4b). Additionally, the expression of some HTGs involved in heat signal transduction, such as *CaM3*, *CNGC8* and *CDPK2*, was down-regulated in Stolwijk Gold, which may adversely affect downstream regulatory processes.

### Analysis of genetic regulatory networks reveals an essential role of HSPs and HSFs in heat resistance

To determine the genetic regulatory networks for heat resistance from the differentially expressed HTGs in the three *Clematis* varieties and to identify hub genes regulating heat resistance, we constructed gene co-expression and protein–protein interaction (PPI) networks (Fig. 5). These networks revealed that HSFs and HSPs, such as HSFA2, HSFB2b, HSP70, and HSP90, played key roles in the heat tolerance of the three *Clematis* varieties. We speculated that the down-regulated expression of many *HSF* and *HSP* (e.g., *HSP70* and *HSP90*) may be the main cause of the sensitivity of Stolwijk Gold to heat stress. Although *C.*

*vitalba* and Polish Spirit were both resistant to heat stress, their genetic regulatory networks for heat resistance varied. Specifically, *C. vitalba* had a relatively small regulatory network, with almost no down-regulated HTGs, whereas Polish Spirit had a relatively large regulatory network with some down-regulated HTGs. Accordingly, there are at least two distinct heat resistance mechanisms in *Clematis* species. Furthermore, analysis of the gene co-expression network revealed several potential targets of heat-responsive transcription factors, including HSFs, DREB2A, and NAC019. The identified gene targets may be useful for future investigations on the heat resistant mechanism in *Clematis* species.

### Differences in expression levels of the HSF and HSP genes is correlated to heat resistance in three Clematis varieties

Considering the importance of HSFs and HSPs for plant heat resistance, we analyzed the phylogenetic relationships of *HSF* and *HSP* genes and compared their expression levels to further characterize the differentially expressed *HSF* and *HSP* genes among three *Clematis* varieties (Fig. 6). The differentially expressed *HSF* genes were divided into three clades. Expression of Clade 1 genes and *PSHSFA1a* and *SGHSFA5* of Clade 2 was down-regulated by heat, suggesting these genes do not induce heat tolerance. All of the *CvHSF* genes were within Clades 2 and 3, and their expression was induced by heat, suggested that HSFs are related to heat tolerance of *C. vitalba*. Clade 3 were generally expressed with a higher level than Clade 2. Thus, heat stress differentially affects the expression of *HSF* genes in different phylogenetic clades. We divided the differentially expressed *HSP* genes into four clades. The 3, 8, and 13 down-regulated *HSP* genes in *C. vitalba*, Polish Spirit, and Stolwijk Gold were mainly clustered in Clades 1, 2, and 3, respectively. The expression levels of most of the *HSP* gene family members in Clade 4 were up-regulated, indicating this clade is important for the heat tolerance of *Clematis* varieties. The down-regulated expression of many *SGHSP* genes following the heat treatment may be related to the sensitivity of Stolwijk Gold to high temperatures. Although the expression of a substantial proportion of the *PSHSP* genes was down-regulated by an exposure to heat, the *HSP* genes were generally more highly expressed in Polish Spirit than in the other two varieties. Furthermore, our analysis revealed a clear expansion of the *HSP* gene family members in Clade 4, which may be beneficial to heat resistance of Polish spirit.

### Classification and characterization of heat shock transcription factors in Clematis vitalba

Considering *C. vitalba* is an original *Clematis* species with a small and efficient heat resistance genetic regulatory network, we predicted it may be useful for breeding. To further classify and characterize the HSFs in *C. vitalba*, we analyzed the phylogenetic relationships, predicted motifs, and expression of *CvHSF* genes. A phylogenetic analysis revealed that Classes A and B each contained three *CvHSF* genes, which were closely related to the orthologous *AtHSF* genes (Fig. 7a). On the basis of the PPI network, gene co-expression network, and expression profiles, *CvHSFA2-1*, *CvHSFA2-2* and *CvHSFB2b* were identified as hub genes critical for the heat tolerance of *C. vitalba*. Meanwhile, to clarify the differences between the HSFs in Classes A and B, the expression of these three genes was analyzed by qRT-PCR. An examination of the predicted motifs revealed that CvHSFA2 and CvHSFB2b have similar N-terminals, but diverse C-terminals, indicative of functional differences between these two HSFs. As representative HSFs of Classes A and B, CvHSFA2-2 has two activator peptide motifs (AHA motifs) and a nuclear export signal at the C-terminal, whereas CvHSFB2b has a repressor domain (Fig. 7b). The qRT-PCR data revealed the increasing *CvHSFA2-1* and *CvHSFA2-2* expression levels in the first 3 h after a high-temperature treatment (38 °C). Moreover, both genes were more highly expressed than *CvHSFB2b*, suggesting that the *HSF* genes in Class A are important for the heat tolerance of *Clematis* species (Fig. 7c).

### CvHSFA2-2 enhanced the viability of E. coli, yeast and tobacco to survive in thermal stress

Based on the above analysis, *CvHSFA2-2* was critical for the heat tolerance of *C. vitalba*. Consequently, we chose *CvHSFA2-2* to verify whether it can endow different host with high temperature resistance. Firstly, *CvHSFA2-2* was cloned and transformed in to *E. coli* BL21 (DE3). At 37 °C, the growth curve and the colony after Z-line of the transgenic *E.coli* were consistent with those of the control group, indicating that the growth of *E.coli* transformed with *CvHSFA2-2* was not affected (Fig. S4). Under 42 °C and 50 °C treatment, the growth of *E. coli* transformed with *CvHSFA2-2* was significantly better than that of the control (Fig. 8a; Fig. 8b). The results showed that *CvHSFA2-2* can significantly improve the heat resistance of *E.coli.* In order to further verify the function of *CvHSFA2-2*, we constructed *CvHSFA2-2* with yeast expression vector pGADT7 and transformed the recombined plasmid into yeast AH109. There was no obvious difference in growth between strain harboring *CvHSFA2-2* and the control (Fig. S4). Under heat stress of 37°C and 42°C, AH109 strain harboring *CvHSFA2-2* grew better and had higher survival rate compared

with the control (Fig. 8c, Fig. 8d). The results showed that *CvHSFA2-2* could improve heat tolerance in yeast AH109 by heterologous expression. Furthermore, we used tobacco rattle virus (TRV)-mediated virus-induced gene silencing (VIGS) to silence the homologous genes of *CvHSFA2-2* in *N. benthamiana*. *HSFA2-2* expression in newly born leaves of *N. benthamiana* significantly decreased after inoculation (Fig. 8e). After heat treatment at 38 ℃ for 3 hours, TRV- *NbHSFA2-2* transgenic line showed perfect heat sensitive phenotype compared with TRV-GFP (Fig. 8f). By NBT and DAB staining, it was found that TRV-*NbHSFA2-2* transgenic tobacco accumulated more ROS than TRV-GFP (Fig. 8g), that is, the contents of superoxide dismutase and peroxidase in TRV-*NbHSFA2-2* were higher than those in TRV-GFP. The result indicated that silence of *NbHSFA2-2* improved heat sensitivity in *N. benthamiana*. All these results verified that *CvHSFA2-2* played an important role in heat tolerance.

# Discussion

Heat is a major abiotic stress that plants have to adequately deal with (Li et al. 2018b; Zhang et al. 2019; Ding et al. 2020). The mechanism regulating the heat tolerance of *Clematis* species remains relatively uncharacterized, which is in contrast to the available information regarding the corresponding mechanisms in traditional model plant species, including *A. thaliana* and *Oryza sativa*. In this study, we first elucidated the molecular basis for the differences in the heat tolerance of three *Clematis* varieties based on a transcriptomic analysis of plant leaves under normal and heat stress conditions. GO enrichment analyses revealed that heat stress mainly influences components of biological membrane and two heat-tolerant *Clematis* varieties have obvious positive regulation to heat stress whereas the heat-sensitive *Clematis* variety does not. Then we identified HTGs and compared their expression levels during various regulatory activities (heat signal transduction, transcription regulation, protein homeostasis, ROS homeostasis and RNA homeostasis) (Table 1, Fig. 4b). Compared with Polish Spirit, there were fewer differentially expressed HTGs, but more down-regulated HTGs, in Stolwijk Gold, which may help to explain the sensitivity of Stolwijk Gold to high temperatures. Although *C. vitalba* and Polish Spirit were both confirmed as heat-tolerant varieties, the underlying mechanisms differed. Although *C. vitalba* had fewer differentially expressed HTGs than Polish Spirit, nearly all of the differentially expressed *CvHTG* genes were up-regulated. In contrast, Polish Spirit had more differentially expressed HTGs, it also had a greater proportion of down-regulated differentially expressed HTGs compared with *Clematis vitalba* (Fig. 4a). Additionally, the differentially expressed HTGs in *C. vitalba* were associated with transcriptional regulation and protein homeostasis, but not heat signal transduction and ROS homeostasis (Fig. 4b). This suggests that *C. vitalba* may quickly respond to heat stress by modulating the activities of intracellular proteins. Moreover, heat stress does not substantially affect the ROS content of *C. vitalba* (Fig. 1c and d), likely because of changes to transcriptional regulation and protein homeostasis. The *C. vitalba* characteristics related to heat resistance may be relevant for breeding new varieties of *Clematis* species.

Gene co-expression and PPI networks revealed the core HSFs and HSPs contributing to the heat stress resistance of *Clematis* species (Fig. 5). Considering the importance of HSFs and HSPs for heat resistance, we analyzed the phylogenetic relationships of the differentially expressed *HSF* and *HSP* genes in three *Clematis* varieties. The diversity in the phylogenetic relationships among the differentially expressed *HSF* and *HSP* genes (Fig. 6) may be associated with the observed differences in heat resistance among the *Clematis* varieties. Orthologous family members often had similar expression profiles (Fig. 6). Notably, we detected a clear expansion of the Clade 4 *HSP* gene cluster in Polish Spirit, which may have influenced the heat resistance of this variety. The related genes should be further analyzed in the future. It is unclear why the expression levels of some *HSF* and *HSP* genes were down-regulated in Polish Spirit and even more so in Stolwijk Gold following the heat treatment. According to previous researches, calcium ($Ca^{2+}$) signaling, ROS signaling, NO signaling and their considerable crosstalk with each other make a difference in heat signal transduction of plant (Liu et al. 2003; Finka et al. 2012; Wang et al. 2015; Gao et al. 2012; Choudhury et al. 2017; Yao et al. 2017; Petrov et al. 2015; Xuan et al. 2010; Karpets et al. 2015; Niu and Liao 2016; Shi et al. 2015; Wu et al. 2015; Hussain et al. 2016). For example, CaM is one of the most important intracellular $Ca^{2+}$ receptors. Knocking out the expression of *AtCaM3* made the resulting mutant more susceptible to HS stress, whereas the overexpression of *AtCaM3* resulted in enhanced plant thermotolerance (Zhang et al. 2009; Liu et al. 2008). We speculated that the down-regulated expression of HTGs related to heat signal transduction (e.g., *CAM3*, *CNGC8* and *CDPK2*) may be an important reason for heat sensitiveness of Stolwijk Gold (Table 1, Fig. 4b). A more thorough functional characterization of these genes may further clarify the mechanism regulating the responses of Polish Spirit and Stolwijk Gold plants to heat stress.

Because of the obvious heat resistance of *C. vitalba*, the differentially expressed *CvHSF* genes were further classified, characterized and verified. *CvHSFA2-2* enhance the viability of E. coli, yeast and tobacco to survive in thermal stress (Fig. 8). Plant HSF family members can be divided into three classes: HSFA, HSFB, and HSFC (Scharf et al. 2018). The differentially expressed *CvHSF* genes identified in this study are *HSFA* and *HSFB* genes. We examined *CvHSFA2-1*, *CvHSFA2-2*, and *CvHSFB2b* to predict the encoded motifs (Fig. 7b). Accordingly, we determined that CvHSFA2-1 and CvHSFA2-2 are A2-type HSFs, whereas CvHSFB2b is a B2-type HSF. Of the HSFA1s-targeted transcription factors/co-activators, HSFA2 is a key regulator of plant thermotolerance (Ogawa et al. 2007; Charng et al. 2007). A qRT-PCR experiment revealed the considerable increase in the *CvHSFA2-1* and *CvHSFA2-2* expression levels in the first 3 h following a high-temperature treatment (Fig. 7c), which is consistent with the results of previous research on other plants(Ding et al. 2020). Therefore, these two *HSF* genes are likely important for the heat resistance of *C. vitalba*. Additionally, a phylogenetic analysis indicated *CvHSFB2b* is an ortholog of *AtHSFB2b* (Fig. 7a). Earlier research proved that AtHSFB2b represses the expression of heat-inducible *HSF* genes, but positively regulates thermotolerance (Ikeda et al. 2011). Hence, CvHSFB2b may be relevant for the molecular breeding of heat-resistant *Clematis* varieties.

Taken together, in this research, a heat-sensitive *Clematis* variety (*Clematis alpina* 'Stolwijk Gold') and two heat-tolerant *Clematis* varieties (*Clematis vitalba* and *Clematis viticella* 'Polish Spirit') were identified according to primary heat-related physiological indices before and after a high-temperature treatment. Gene expression profiles of three *Clematis* varieties under normal and high temperature based on transcriptome data were reported, which provided valuable resources for the research of *Clematis* species. Moreover, we compared the varieties regarding their responses to heat to clarify the differences in their heat resistance based on HTGs that we identified. Furthermore, to characterize the considerable heat resistance of *C. vitalba*, we identified two HSF classes with various functions related to heat resistance. By heterologous expression and VIGS, we found CvHSFA2-2 significantly enhanced the viability of E. coli, yeast and tobacco to survive in thermal stress. Our study provided first insights into the diversity of heat response mechanisms of *Clematis* species, with implications for the breeding of heat-resistant and ornamental *Clematis* varieties.

# Abbreviations

HTGs: heat tolerance-related genes; PPI: protein–protein interaction; HSFs: heat shock transcription factors; HSPs: heat shock proteins; TIR1: TRANSPORT INHIBITOR RESPONSE 1; ROS: reactive oxygen species; Cv: *Clematis vitalba*; PS: Polish Spirit SG: Stolwijk Gold; HT: high-temperature; SOD: superoxide dismutase activity; DEGs: differentially expressed genes; AHA motifs: activator peptide motifs; MDA: Malondialdehyde; NBT: Nitro blue tetrazole; DAB: Diaminobenzidine; GO: Gene Ontology; KEGG: Kyoto Encyclopedia of Genes and Genomes; RC: relative conductivity; RWC: relative water content; TRV: tobacco rattle virus; VIGS: virus-induced gene silencing

# Declarations

### Ethics approval and consent to participate

Not applicable

### Consent for publication

Not applicable

### Availability of data and materials

The datasets supporting the conclusions of this article are included within the article and its supplementary information files. The RNA-seq data are available from NCBI of sequence Read Archive (SRA project: PRJNA664279).

### Competing interests

The authors declare that they have no competing interests in this paper.

### Funding

This work was supported by Science and Technology Commission of Shanghai Municipality (Grant No. 18DZ2283500), Shanghai Engineering Research Center of Plant Germplasm Resources (17DZ2252700), Science and Technology Commission of Shanghai Municipality (18DZ2260500), Shanghai Key Laboratory of Plant Molecular Sciences and National Key R&D Program of China (2018YFD1000400). The funding sources were not involved in any process of this study.

### Author Contributions

FM and HZ conceived the project and designed the study; HZ conducted transcriptome analysis based on RNA-seq. CJ , HZ, JM and LZ collected the samples. HZ, RW, LZ, RG, SP and YZ performed physiological experiments, qRT-PCR and function verification; HZ wrote the manuscript; YL, JM and CM contributed to the discussion of the manuscript. FM, ZH and SF revised the manuscript. All of the authors discussed the results and commented on the manuscript.

### Acknowledgements

We thank France Jardin Botanique for providing seeds of three Clematis varieties and Liwen Bianji, Edanz Editing China (www.liwenbianji.cn/ac) for editing the English text of a draft of this manuscript.

## References

Assenov Y, Ramirez F, Schelhorn SE, Lengauer T, Albrecht M (2008) Computing topological parameters of biological networks. Bioinformatics 24 (2):282-284. doi:10.1093/bioinformatics/btm554

Bao G, Tang W, An Q, Liu Y, Tian J, Zhao N, Zhu S (2020) Physiological effects of the combined stresses of freezing-thawing, acid precipitation and deicing salt on alfalfa seedlings. BMC Plant Biol 20 (1):204. doi:10.1186/s12870-020-02413-4

Bao G, Zhang M, Li Y, Chang Y, Tang W, Zhu S, Fan C, Ding X (2019) Physiological responses of alfalfa seedings to freeze-thaw cycles and alkaline salt stress. Fresenius Environmental Bulletin 28 (5):4114-4122

Cen WJ, Liu JB, Lu SY, Jia PL, Yu K, Han Y, Li RB, Luo JJ (2018) Comparative proteomic analysis of QTL CTS-12 derived from wild rice (*Oryza rufipogon Griff.*), in the regulation of cold acclimation and de-acclimation of rice (*Oryza sativa L.*) in response to severe chilling stress. BMC Plant Biol 18:17. doi:10.1186/s12870-018-1381-7

Charng YY, Liu HC, Liu NY, Chi WT, Wang CN, Chang SH, Wang TT (2007) A heat-inducible transcription factor, HsfA2, is required for extension of acquired thermotolerance in Arabidopsis. Plant Physiology 143 (1):251-262. doi:10.1104/pp.106.091322

Choudhury FK, Rivero RM, Blumwald E, Mittler R (2017) Reactive oxygen species, abiotic stress and stress combination. Plant J 90 (5):856-867. doi:10.1111/tpj.13299

Ding YL, Shi YT, Yang SH (2020) Molecular regulation of plant responses to environmental temperatures. Molecular Plant 13 (4):544-564. doi:10.1016/j.molp.2020.02.004

Fang YJ, Liao KF, Du H, Xu Y, Song HZ, Li XH, Xiong LZ (2015) A stress-responsive NAC transcription factor SNAC3 confers heat and drought tolerance through modulation of reactive oxygen species in rice. J Exp Bot 66 (21):6803-6817. doi:10.1093/jxb/erv386

Felsenstein J (1985) Confidence limits on phylogenies: an approach using the bootstrap. Evolution; international journal of organic evolution 39 (4):783-791. doi:10.1111/j.1558-5646.1985.tb00420.x

Finka A, Cuendet AFH, Maathuis FJM, Saidi Y, Goloubinoff P (2012) Plasma membrane cyclic nucleotide gated calcium channels control land plant thermal sensing and acquired thermotolerance. Plant Cell 24 (8):3333-3348. doi:10.1105/tpc.112.095844

Flexas J, Ribas-Carbo M, Bota J, Galmes J, Henkle M, Martinez-Canellas S, Medrano H (2006) Decreased Rubisco activity during water stress is not induced by decreased relative water content but related to conditions of low stomatal conductance and chloroplast CO2 concentration. New Phytol 172 (1):73-82. doi:10.1111/j.1469-8137.2006.01794.x

Gao F, Han XW, Wu JH, Zheng SZ, Shang ZL, Sun DY, Zhou RG, Li B (2012) A heat-activated calcium-permeable channel Arabidopsis cyclic nucleotide-gated ion channel 6 is involved in heat shock responses. Plant Journal 70 (6):1056-1069. doi:10.1111/j.1365-313X.2012.04969.x

Guan QM, Yue XL, Zeng HT, Zhu JH (2014) The protein phosphatase rcf2 and its interacting partner nac019 are critical for heat stress-responsive gene regulation and thermotolerance in Arabidopsis. Plant Cell 26 (1):438-453. doi:10.1105/tpc.113.118927

Hendrick JP, Hartl FU (1993) Molecular chaperone functions of heat-shock proteins. Annual review of biochemistry 62:349-384. doi:10.1146/annurev.bi.62.070193.002025

Huang YC, Niu CY, Yang CR, Jinn TL (2016) The heat stress factor HSFA6b connects ABA signaling and ABA-Mediated heat responses. Plant Physiology 172 (2):1182-1199. doi:10.1104/pp.16.00860

Hussain A, Mun BG, Imran QM, Lee SU, Adamu TA, Shahid M, Kim KM, Yun BW (2016) Nitric oxide mediated transcriptome profiling reveals activation of multiple regulatory pathways in *Arabidopsis thaliana*. Front Plant Sci 7:18. doi:10.3389/fpls.2016.00975

Ikeda M, Mitsuda N, Ohme-Takagi M (2011) Arabidopsis HsfB1 and HsfB2b act as repressors of the expression of heat-inducible hsfs but positively regulate the acquired thermotolerance. Plant Physiology 157 (3):1243-1254. doi:10.1104/pp.111.179036

Jones DT, Taylor WR, Thornton JM (1992) The rapid generation of mutation data matrices from protein sequences. Computer applications in the biosciences : CABIOS 8 (3):275-282. doi:10.1093/bioinformatics/8.3.275

Karpets Y, Kolupaev Y, Vayner A (2015) Functional interaction between nitric oxide and hydrogen peroxide during formation of wheat seedling induced heat resistance. Russ J Plant Physiol 62 (1):65-70. doi:10.1134/s1021443714060090

Kumar S, Stecher G, Li M, Knyaz C, Tamura K (2018) MEGA X: molecular evolutionary genetics analysis across computing platforms. Molecular Biology and Evolution 35 (6):1547-1549. doi:10.1093/molbev/msy096

Kumar SV, Lucyshyn D, Jaeger KE, Alos E, Alvey E, Harberd NP, Wigge PA (2012) Transcription factor PIF4 controls the thermosensory activation of flowering. Nature 484 (7393):242-U127. doi:10.1038/nature10928

Kumar SV, Wigge PA (2010) H2A.Z-containing nucleosomes mediate the thermosensory response in Arabidopsis. Cell 140 (1):136-147. doi:10.1016/j.cell.2009.11.006

Legris M, Klose C, Burgie ES, Rojas CC, Neme M, Hiltbrunner A, Wigge PA, Schafer E, Vierstra RD, Casal JJ (2016) Phytochrome B integrates light and temperature signals in Arabidopsis. Science 354 (6314):897-900. doi:10.1126/science.aaf5656

Li B, Gao K, Ren H, Tang W (2018a) Molecular mechanisms governing plant responses to high temperatures. J Integr Plant Biol 60 (9):757-779. doi:10.1111/jipb.12701

Li XR, Deb J, Kumar SV, Ostergaard L (2018b) Temperature modulates tissue-specification program to control fruit dehiscence in Brassicaceae. Molecular Plant 11 (4):598-606. doi:10.1016/j.molp.2018.01.003

Liu H-T, Gao F, Li G-L, Han J-L, De-Long L, Sun D-Y, Zhou R-G (2008) The calmodulin-binding protein kinase 3 is part of heat-shock signal transduction in *Arabidopsis thaliana*. Plant Journal 55 (5):760-773. doi:10.1111/j.1365-313X.2008.03544.x

Liu H-T, Li B, Shang Z-L, Li X-Z, Mu R-L, Sun D-y, Zhou R-g (2003) Calmodulin is involved in heat shock signal transduction in wheat. Plant Physiology (Rockville) 132 (3):1186-1195. doi:10.1104/pp.102.018564

Liu HC, Charng YY (2013) Common and distinct functions of Arabidopsis class A1 and A2 heat shock factors in diverse abiotic stress responses and development. Plant Physiology 163 (1):276-290. doi:10.1104/pp.113.221168

Liu HC, Liao HT, Charng YY (2011) The role of class A1 heat shock factors (HSFA1s) in response to heat and other stresses in Arabidopsis. Plant Cell Environ 34 (5):738-751. doi:10.1111/j.1365-3040.2011.02278.x

Liu Q, Kasuga M, Sakuma Y, Abe H, Miura S, Yamaguchi-Shinozaki K, Shinozaki K (1998) Two transcription factors, DREB1 and DREB2, with an EREBP/AP2 DNA binding domain separate two cellular signal transduction pathways in drought- and low-temperature-responsive gene expression, respectively, in Arabidopsis. The Plant cell 10 (8):1391-1406. doi:10.2307/3870648

Livak KJ, Schmittgen TD (2001) Analysis of relative gene expression data using real-time quantitative PCR and the 2(-Delta Delta C(T)) Method. Methods (San Diego, Calif) 25 (4):402-408. doi:10.1006/meth.2001.1262

Minh BQ, Schmidt HA, Chernomor O, Schrempf D, Woodhams MD, von Haeseler A, Lanfear R (2020) IQ-TREE 2: new models and efficient methods for phylogenetic inference in the genomic era. Molecular Biology and Evolution 37 (5):1530-1534. doi:10.1093/molbev/msaa015

Niu LJ, Liao WB (2016) Hydrogen peroxide signaling in plant development and abiotic responses: crosstalk with nitric oxide and calcium. Front Plant Sci 7:14. doi:10.3389/fpls.2016.00230

Ogawa D, Yamaguchi K, Nishiuchi T (2007) High-level overexpression of the Arabidopsis HsfA2 gene confers not only increased themotolerance but also salt/osmotic stress tolerance and enhanced callus growth. J Exp Bot 58 (12):3373-3383. doi:10.1093/jxb/erm184

Paynter Q, Waipara N, Peterson P, Hona S, Fowler S, Gianotti A, Wilkie P (2006) The impact of two introduced biocontrol agents, *Phytomyza vitalbae* and *Phoma clematidina*, on *Clematis vitalba* in New Zealand. Biological Control 36 (3):350-357. doi:10.1016/j.biocontrol.2005.09.011

Petrov V, Hille J, Mueller-Roeber B, Gechev TS (2015) ROS-mediated abiotic stress-induced programmed cell death in plants. Front Plant Sci 6:16. doi:10.3389/fpls.2015.00069

Picciau R, Porceddu M, Bacchetta G (2017) Can alternating temperature, moist chilling, and gibberellin interchangeably promote the completion of germination in *Clematis vitalba* seeds? Botany 95 (8):847-852. doi:10.1139/cjb-2017-0039

Qiao B, Zhang Q, Liu DL, Wang HQ, Yin JY, Wang R, He ML, Cui M, Shang ZL, Wang DK, Zhu ZG (2015) A calcium-binding protein, rice annexin OsANN1, enhances heat stress tolerance by modulating the production of H2O2. J Exp Bot 66 (19):5853-5866. doi:10.1093/jxb/erv294

Redmond CM, Stout JC (2018) Breeding system and pollination ecology of a potentially invasive alien *Clematis vitalba L.* in Ireland. Journal of Plant Ecology 11 (1):56-63. doi:10.1093/jpe/rtw137

Sato H, Mizoi J, Tanaka H, Maruyama K, Qin F, Osakabe Y, Morimoto K, Ohori T, Kusakabe K, Nagata M, Shinozaki K, Yamaguchi-Shinozaki K (2014) Arabidopsis DPB3-1, a DREB2A interactor, specifically enhances heat stress-induced gene expression by forming a heat stress-specific transcriptional complex with NF-Y subunits. Plant Cell 26 (12):4954-4973. doi:10.1105/tpc.114.132928

Scharf KD, Berberich T, Ebersberger I, Nover L (2018) The plant heat stress transcription factor (Hsf) family: Structure, function and evolution (vol 1819, pg 104, Year 2017). Biochim Biophys Acta-Gene Regul Mech 1861 (1):60-60. doi:10.1016/j.bbagrm.2017.12.005

Schramm F, Larkindale J, Kiehlmann E, Ganguli A, Englich G, Vierling E, von Koskull-Doring P (2008) A cascade of transcription factor DREB2A and heat stress transcription factor HsfA3 regulates the heat stress response of Arabidopsis. Plant J 53 (2):264-274. doi:10.1111/j.1365-313X.2007.03334.x

Shannon P, Markiel A, Ozier O, Baliga NS, Wang JT, Ramage D, Amin N, Schwikowski B, Ideker T (2003) Cytoscape: A software environment for integrated models of biomolecular interaction networks. Genome Research 13 (11):2498-2504. doi:10.1101/gr.1239303

Shi CY, Qi C, Ren HY, Huang AX, Hei SM, She XP (2015) Ethylene mediates brassinosteroid-induced stomatal closure via G alpha protein-activated hydrogen peroxide and nitric oxide production in Arabidopsis. Plant J 82 (2):280-301. doi:10.1111/tpj.12815

Vacca RA, Valenti D, Bobba A, Merafina RS, Passarella S, Marra E (2006) Cytochrome c is released in a reactive oxygen species-dependent manner and is degraded via caspase-like proteases in tobacco bright-yellow 2 cells en route to heat shock-induced cell death. Plant Physiology 141 (1):208-219. doi:10.1104/pp.106.078683

Wanasinghe DN, Jones EBG, Camporesi E, Boonmee S, Ariyawansa HA, Wijayawardene NN, Mortimer PE, Xu J, Yang J-B, Hyde KD (2014) An exciting novel member of Lentitheciaceae in Italy from *Clematis Vitalba*. Cryptogamie, Mycologie 35 (4):323-337. doi:10.7872/crym.v35.iss4.2014.323

Wang RH, Zhang Y, Kieffer M, Yu H, Kepinski S, Estelle M (2016) HSP90 regulates temperature dependent seedling growth in Arabidopsis by stabilizing the auxin co-receptor F-box protein TI R1 (vol 7, pg 1026, 2016). Nat Commun 7:1. doi:10.1038/ncomms11677

Wang X, Ma XL, Wang H, Li BJ, Clark G, Guo Y, Roux S, Sun DY, Tang WQ (2015) Proteomic study of microsomal proteins reveals a key role for Arabidopsis Annexin 1 in mediating heat stress-induced increase in intracellular calcium levels. Mol Cell Proteomics 14 (3):686-694. doi:10.1074/mcp.M114.042697

Wu D, Chu HY, Jia LX, Chen KM, Zhao LQ (2015) A feedback inhibition between nitric oxide and hydrogen peroxide in the heat shock pathway in Arabidopsis seedlings. Plant Growth Regul 75 (2):503-509. doi:10.1007/s10725-014-0014-x

Xuan Y, Zhou S, Wang L, Cheng YD, Zhao LQ (2010) Nitric oxide functions as a signal and acts upstream of AtCaM3 in thermotolerance in Arabidopsis seedlings. Plant Physiology 153 (4):1895-1906. doi:10.1104/pp.110.160424

Yao Y, He RJ, Xie QL, Zhao XH, Deng XM, He JB, Song L, He J, Marchant A, Chen XY, Wu AM (2017) ETHYLENE RESPONSE FACTOR 74 (ERF74) plays an essential role in controlling a respiratory burst oxidase homolog D (RbohD)-dependent mechanism in response to different stresses in Arabidopsis. New Phytol 213 (4):1667-1681. doi:10.1111/nph.14278

Zhang J, Li XM, Lin HX, Chong K (2019) Crop improvement through temperature resilience. Annu Rev Plant Biol 70:753-780. doi:10.1146/annurev-arplant-050718-100016

Zhang J, Yu DS, Zhang Y, Liu K, Xu KD, Zhang FL, Wang J, Tan GX, Nie XH, Ji QH, Zhao L, Li CW (2017) Vacuum and co-cultivation agroinfiltration of (germinated) seeds results in tobacco rattle virus (TRV) mediated whole-plant virus-induced gene silencing (VIGS) in wheat and maize. Front Plant Sci 8:12. doi:10.3389/fpls.2017.00393

Zhang W, Zhou RG, Gao YJ, Zheng SZ, Xu P, Zhang SQ, Sun DY (2009) Molecular and genetic evidence for the key role of AtCaM3 in heat-shock signal transduction in Arabidopsis. Plant Physiology 149 (4):1773-1784. doi:10.1104/pp.108.133744

# Figures

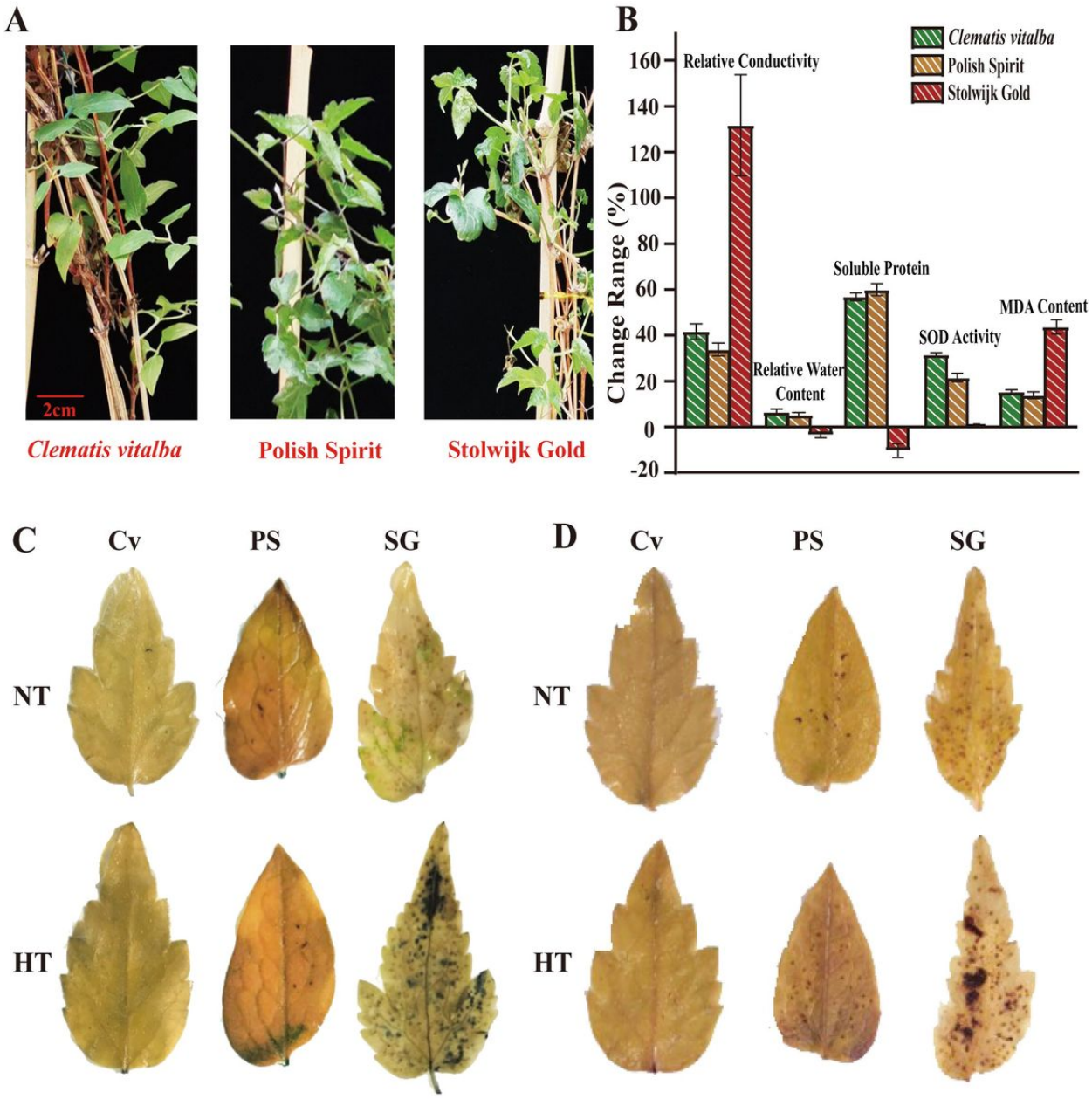


**Figure 1**

Heat shock phenotype and physiological change of three Clematis varieties after high temperature treatment. (a) Phenotype of three Clematis varieties (Clematis vitalba, Clematis viticella 'Polish Spirit' and Clematis alpina 'Stolwijk Gold') after high temperature treatment (38°C for 3 hours). (b) Change of relative conductivity, relative water content, soluble protein, SOD activity and MDA content after high temperature treatment (38°C for 3 hours) among three Clematis varieties. Data were mean ± SE from three biological replicates. (c) NBT staining of three Clematis varieties leaves after normal (22°C) and high (38°C) temperature treatment for 3 hours. (d) DAB staining of three Clematis varieties leaves after normal (22°C) and high (38°C) temperature treatment for 3 hours.

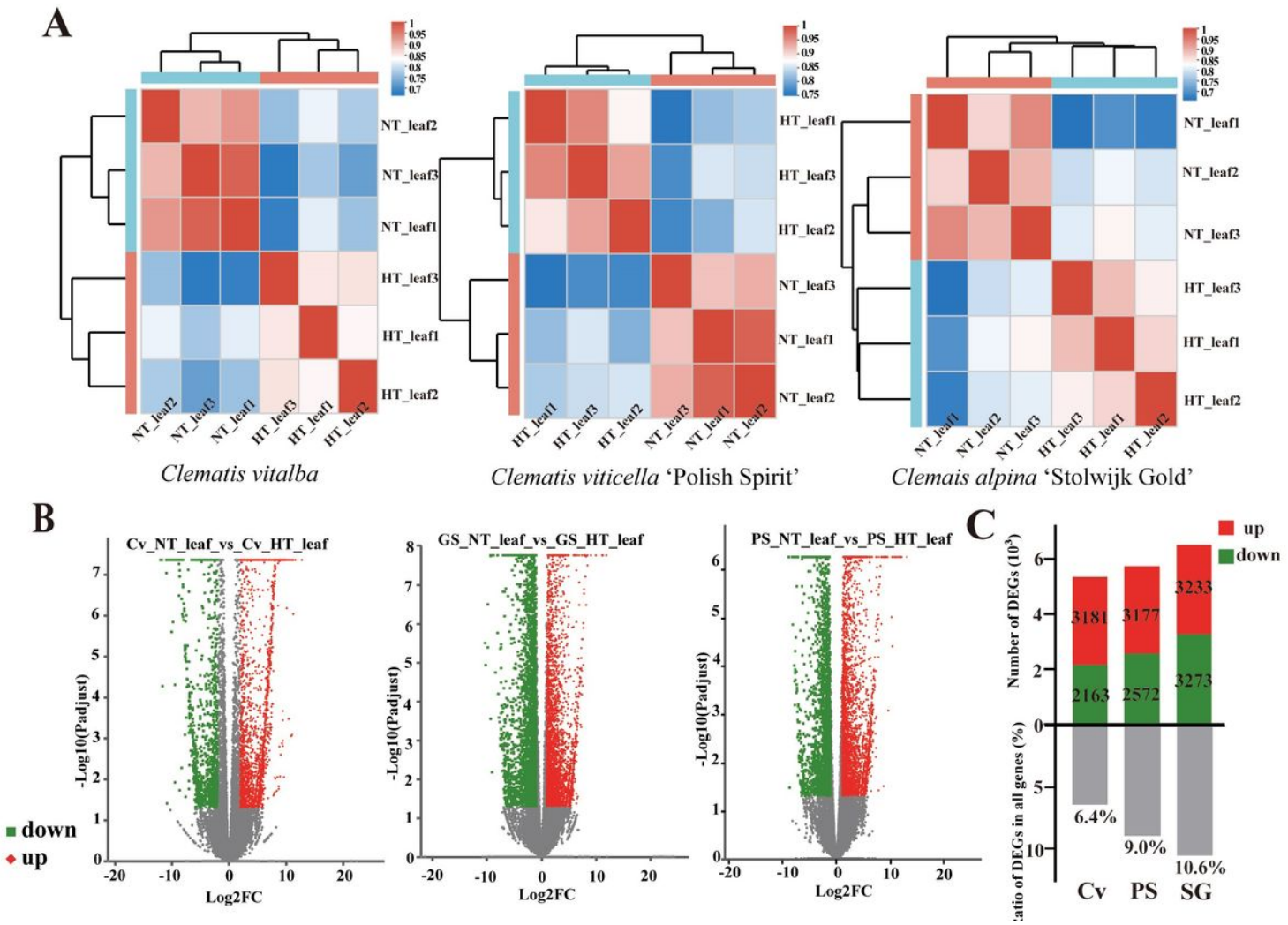


## Figure 2

Correlations among transcriptomes, visualization of differential expression and statistics of differentially expressed genes. (a) Correlation matrix and cluster dendrogram of the whole dataset of the mapped reads. For every Clematis variety, the analysis was performed by comparing the values of the entire transcriptome in all six samples with three biological replicates. Correlation analysis and hierarchical cluster analysis were performed using R software. Red color indicates a stronger correlation and blue weaker. (b) Volcano plots of differential expression of three Clematis varieties under normal and high temperature. Red and green represent “up regulated” and “down regulated”, respectively. (c) Differentially expressed genes’ number and proportion in all genes.

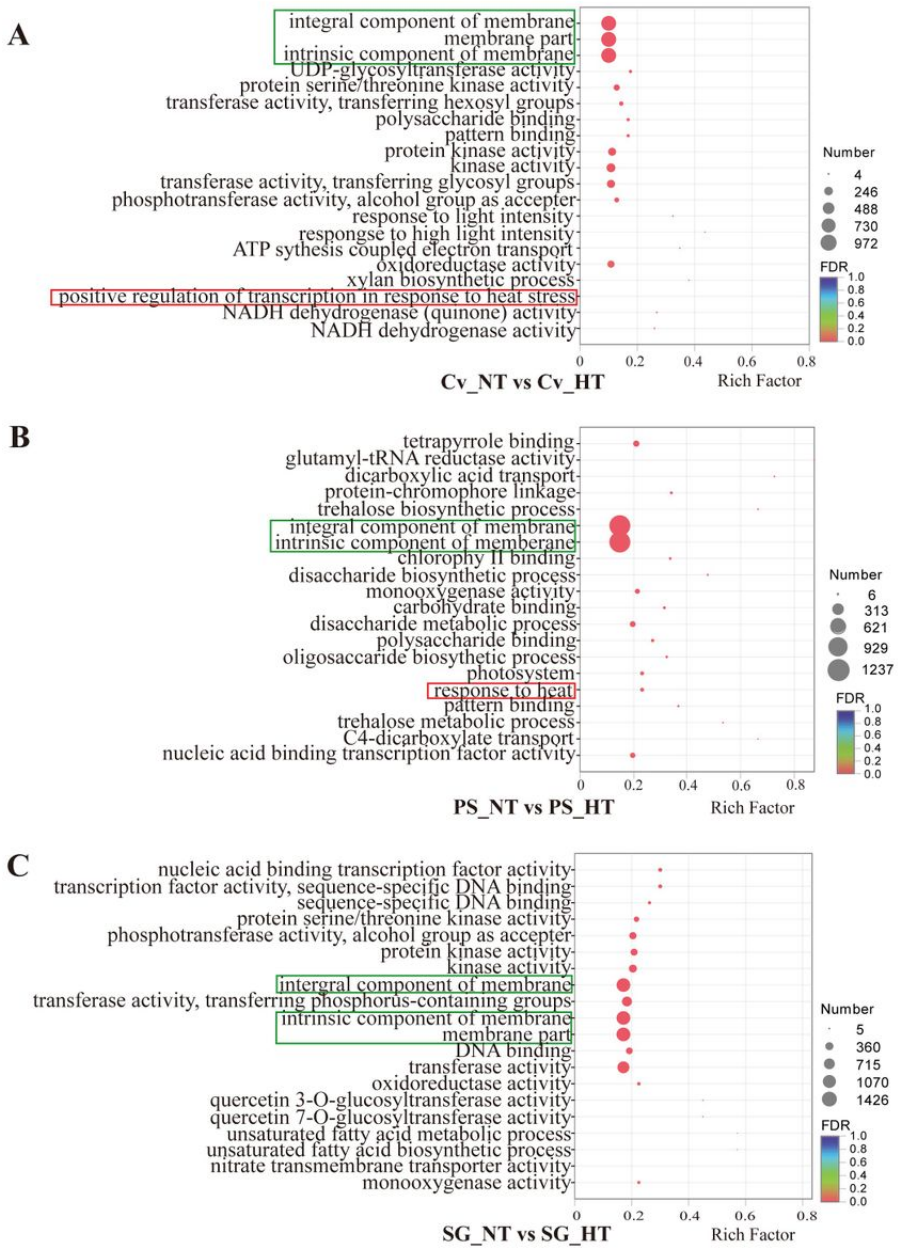


## Figure 3

The GO enrichment analyses of DEGs under normal and high temperature in three Clematis varieties. Top20 of GO enrichment terms of three varieties' DEGs were respectively showed in Fig. 3a, b and c. The GO enrichment terms involved in component of membrane and positive regulation of heat response were labeled in green box and red box, respectively.

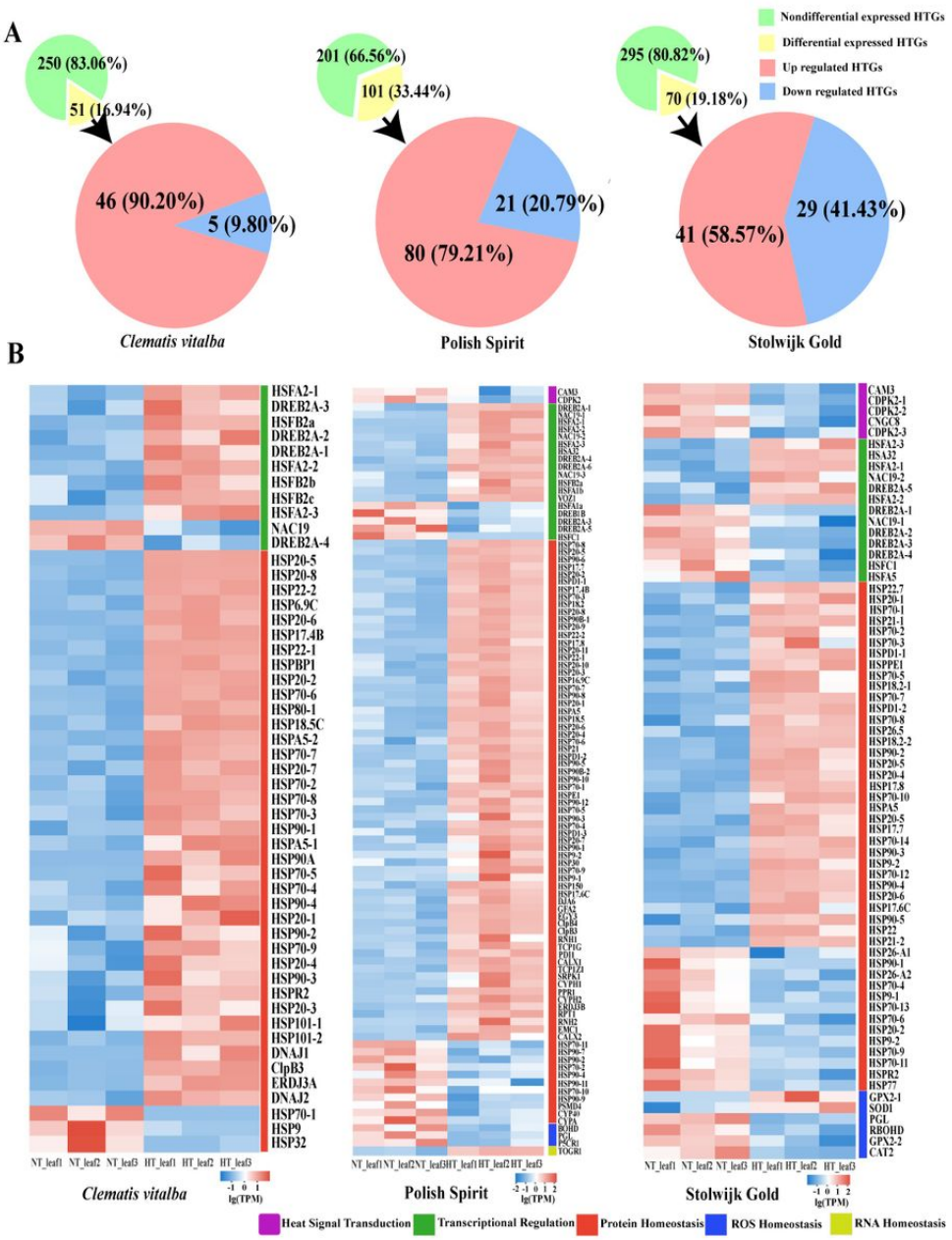


## Figure 4

The proportion of differential expressed HTGs in all HTGs and expression profiles of differentially expressed HTGs in three Clematis varieties. (a) Pie charts of HTGs (nondifferential expressed HTGs, differential expressed HTGs, up regulated HTGs and down regulated HTGs) (b) Heatmap of differentially expressed HTGs belong to different regulation levels (heat signal transduction, transcriptional regulation, protein homeostasis, ROS homeostasis and RNA homeostasis)

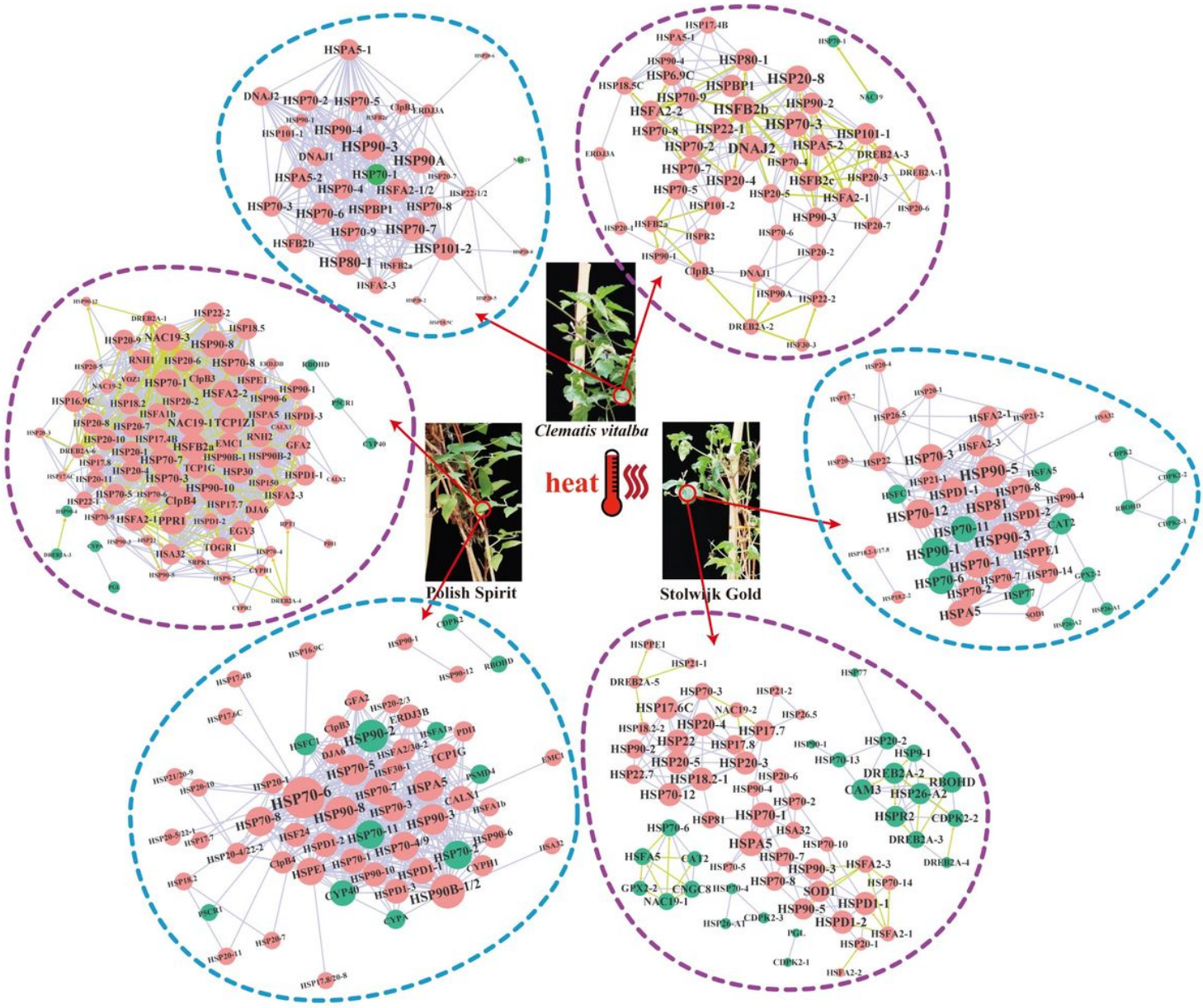


## Figure 5

Heat-related genetic regulatory network of three Clematis varieties. The networks inside dotted purple line and dotted blue line showed gene co-expression and protein-protein interaction (PPI) relationships, respectively. Red nodes and green nodes represented up regulated and down regulated genes respectively. The size of nodes represented number of edges directly connected with nodes. Yellow arrows pointed at potential targets of heat-responsive transcription factors.

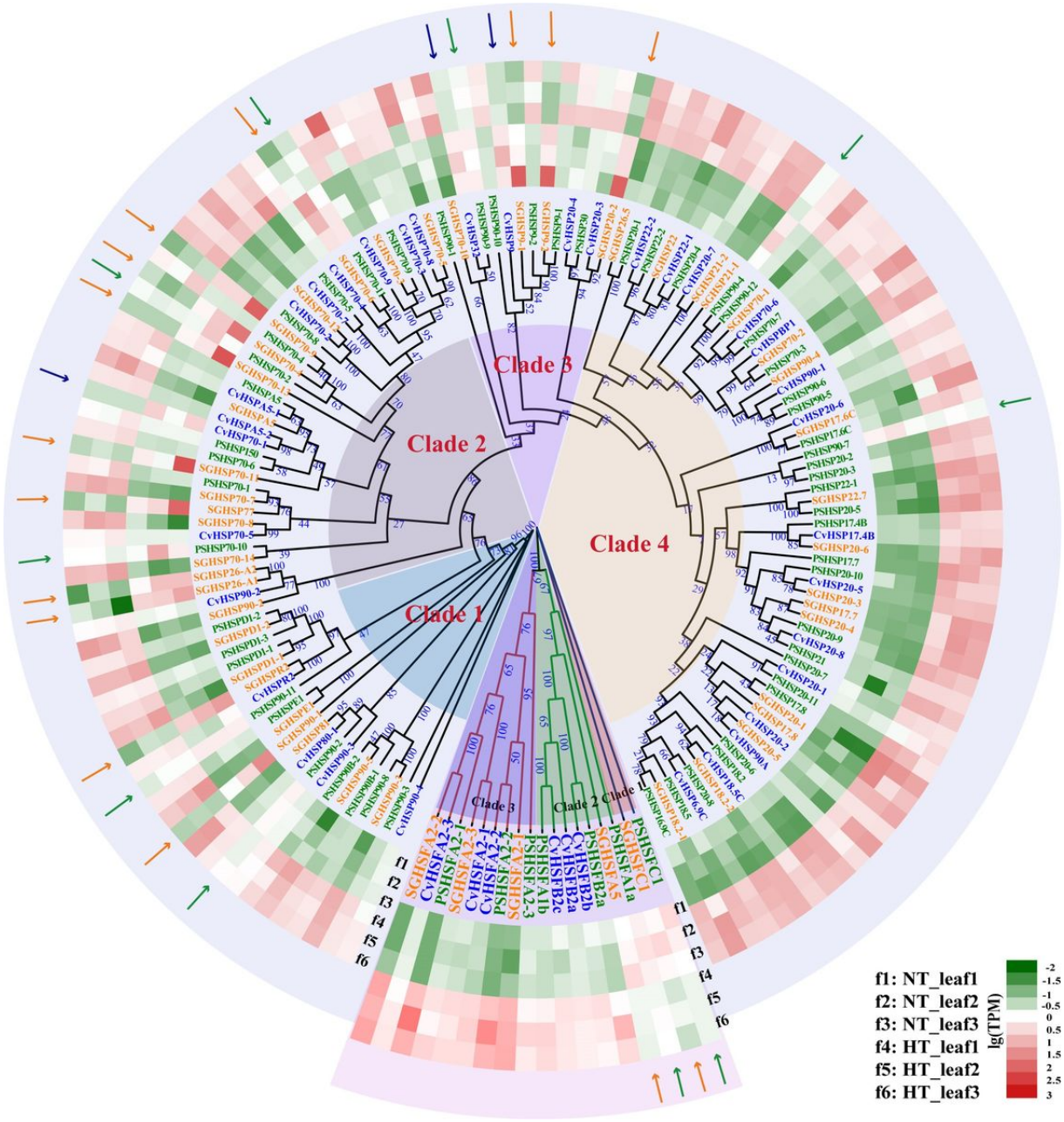


## Figure 6

Phylogenetic analysis and differential expression of HSF genes and HSP genes in three Clematis varieties. The trees of differential expressed HSFs and HSPs were both constructed in IQ-TREE v2.0.6 with JTT+I+G4 and VT+R3 model and could be divided into 3 and 4 clades, respectively. Support rates were labeled at corresponding branches. The heatmap was generated from the TPM data of transcriptomes. Green and red represented “down regulated” and “up regulated” respectively. Blue, green and yellow arrows pointed at down regulated HSFs or HSPs of Clematis vitalba, Polish Spirit and Stolwijk Gold, respectively.

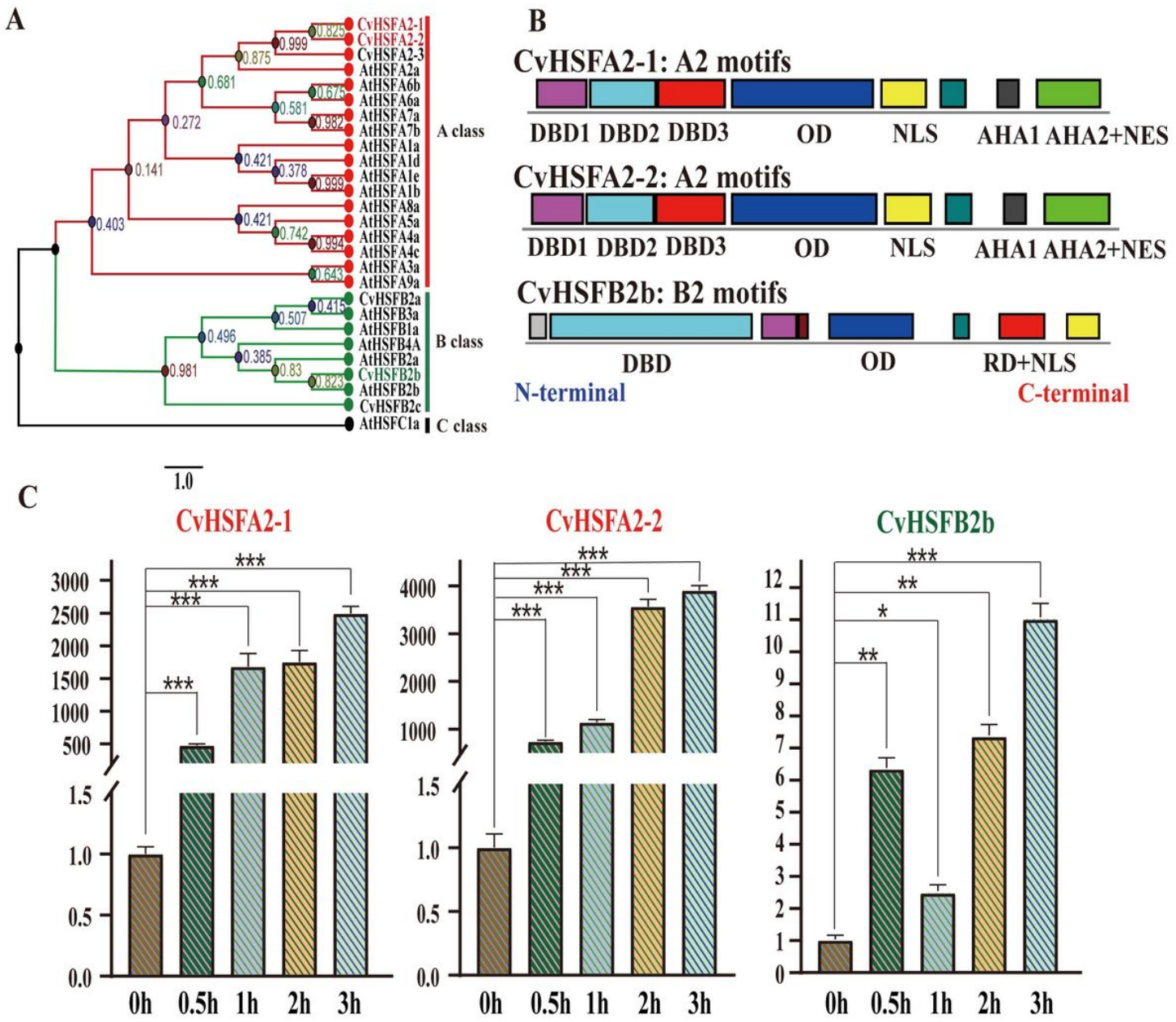


Figure 7

Classification, motifs and qRT-PCR analysis of CvHSFs. (a) Phylogenetic analysis of differential expressed CvHSFs and HSF family members of Arabidopsis thaliana. The tree was constructed in MEGA X using the maximum likelihood method and divided into A, B and C three classes. Support rates were labeled at corresponding branches. (b) Motifs of CvHSFA2-1, CvHSFA2-2 and CvHSFB2b. Motif prediction and visualization were performed in HEATSTER (https://applbio.biologie.uni-frankfurt.de/hsf/heatster/home.php). (c) CvHSFA2-1, CvHSFA2-2 and CvHSFB2b qRT-PCR analysis from leaves of Clematis vitalba after different high temperature treatment times. The expression of CvUBC2D was used as an internal control. Data were mean ± SE from three biological replicates. * indicate statistically significant differences by student t-test: P<0.05. ** P<0.01.

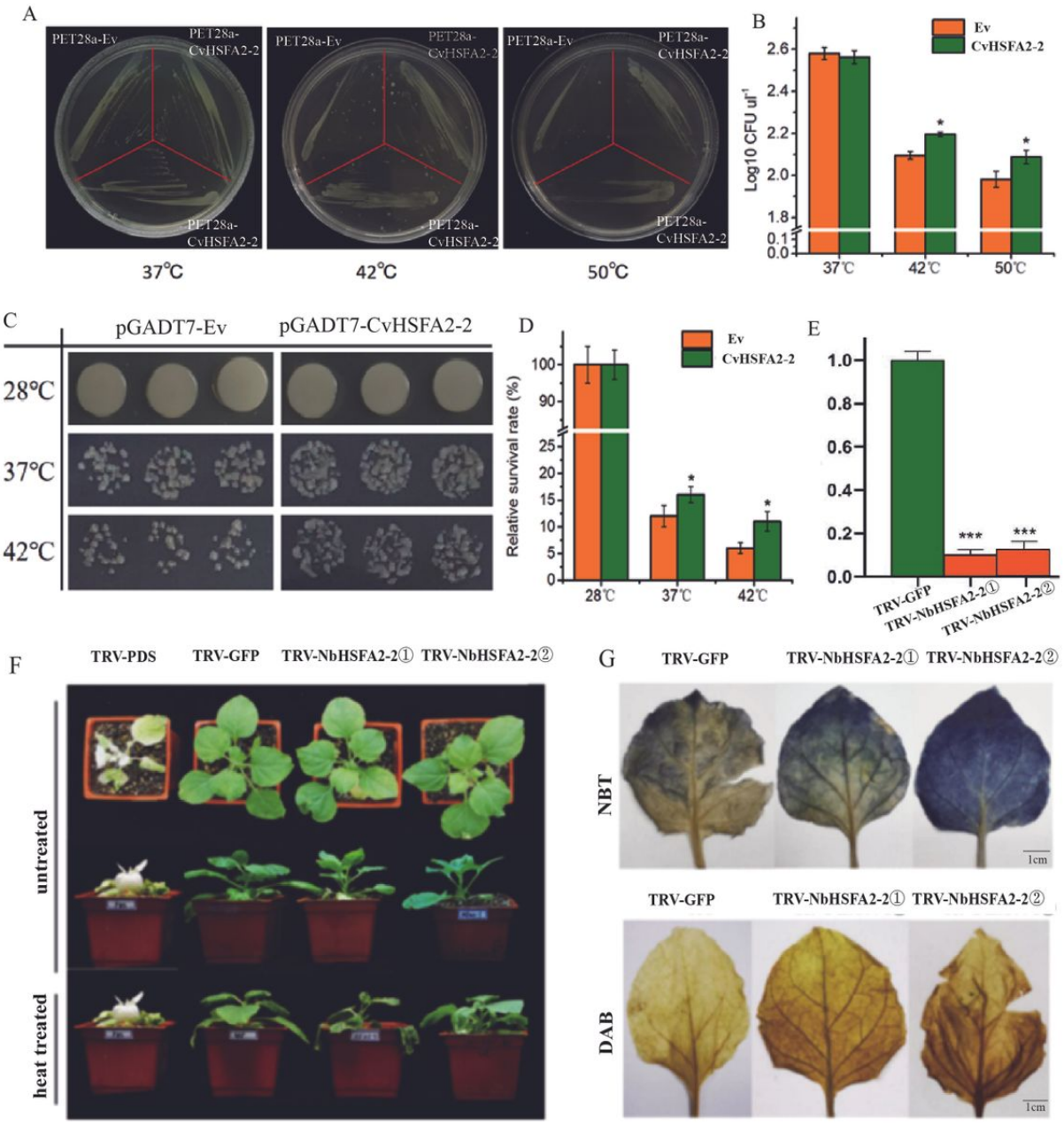


**Figure 8**

Phenotype of E. coli and yeast overexpressing CvHSFA2-2 and tobacco silencing NbHSFA2-2 under heat stress. (a) CvHSFA2-2 transgenic E. coli spot plate grown after 37°C, 42°C or 50 °C treatment,respectively. (b) Colony forming units (cfu) of transgenic E. coli before and after heat shock. Error bars represent the standard error of three biological replicates. *P < 0.05. **P < 0.01. (c) The growth of yeast AH109 harboring pGADT7-EV or pGADT7-CvHSFA2-2 under heat stress. (d) Relative survival rate of yeast AH109 harboring pGADT7-EV or pGADT7-CvHSFA2-2 treated with 37°C or 42°C. (e) Silencing effect of HSF30-2 in N. benthamiana by VIGS, ***P < 0.001. (f) Phenotype of NbHSFA2-2-silencing tobacco by VIGS before and after heat shock (38°C, 3h). TRV-NbHSFA2-2① and TRV-NbHSFA2-2② means two different NbHSFA2-2 silencing lines. (g) DAB and NBT staining of NbHSFA2-2-silencing tobacco after heat treatment.

## Supplementary Files

This is a list of supplementary files associated with this preprint. Click to download.

- Additionalfile1Supplementaryfigure1.jpg

- Additionalfile10SupplementaryTable6.xlsx
- Additionalfile11SupplementaryTable7.xlsx
- Additionalfile12SupplementaryTable8.xlsx
- Additionalfile2Supplementaryfigure2.jpg
- Additionalfile3Supplementaryfigure3.jpg
- Additionalfile4Supplementaryfigure4.jpg
- Additionalfile5SupplementaryTable1.xlsx
- Additionalfile6SupplementaryTable2.docx
- Additionalfile7SupplementaryTable3.docx
- Additionalfile8SupplementaryTable4.xlsx
- Additionalfile9SupplementaryTable5.docx
- SupplementaryInformation.docx